Structural Engineering and Mechanics, *Vol. 61, No. 6 (2017) 701-709*
DOI: https://doi.org/10.12989/sem.2017.61.6.701

Nonlinear spectral design analysis of a structure for hybrid self-centring device enabled structures

Farzin G. Golzar*, Geoffrey W. Rodgers[a] and J. Geoffrey Chase[b]

Department of Mechanical Engineering, University of Canterbury, Private Bag 4800, Christchurch, New Zealand

(Received February 1, 2016, Revised October 15, 2016, Accepted November 9, 2016)

Abstract. Seismic dissipation devices can play a crucial role in mitigating earthquake damages, loss of life and post-event repair and downtime costs. This research investigates the use of ring springs with high-force-to-volume (HF2V) dissipaters to create damage-free, recentring connections and structures. HF2V devices are passive rate-dependent extrusion-based devices with high energy absorption characteristics. Ring springs are passive energy dissipation devices with high self-centring capability to reduce the residual displacements. Dynamic behaviour of a system with nonlinear structural stiffness and supplemental hybrid damping via HF2V devices and ring spring dampers is used to investigate the design space and potential. HF2V devices are modelled with design forces equal to 5% and 10% of seismic weight and ring springs are modelled with loading stiffness values of 20% and 40% of initial structural stiffness and respective unloading stiffness of 7% and 14% of structural stiffness (equivalent to 35% of their loading stiffness). Using a suite of 20 design level earthquake ground motions, nonlinear response spectra for 8 different configurations are generated. Results show up to 50% reduction in peak displacements and greater than 80% reduction in residual displacements of augmented structure compared to the baseline structure. These gains come at a cost of a significant rise in the base shear values up to 200% mainly as a result of the force contributed by the supplemental devices.

Keywords: spectral design; self-centring; nonlinear structure; high force damper

1. Introduction

Structures are subjected to a significant amount of energy input during a short period of earthquake ground motion resulting in damage to structural and non-structural components (Chang 2010, Yon *et al.* 2013). Minimizing this damage and the associated financial and social consequences is a key goal in the design of modern low-damage structures. Seismic design to date is mainly focused on developing sacrificial designs to dissipate energy and ensure life safety. However, the costs associated with long interruptions to serviceability and repair, or even total demolition of the structure following a severe earthquake result in major financial losses that significantly impact the community (Kaiser *et al.* 2012). Hence, there is an increasing demand for structural resilience through damage resistant structural designs that dissipate energy without sacrificial damage.

Damage Avoidance Design (DAD) is a relatively new design philosophy gaining acceptance among structural engineers (Mander and Cheng 1997, Hamid and Mander 2014). Its overall goal is to design low- to no- damage structures with decreased post-earthquake repairs, and minimal disruptions, to substantially lower the economic and business costs of earthquakes. To achieve Damage Avoidance Design, energy dissipaters used in the structure must be capable of performing in a consistent and repeatable manner with minimal degradation over the life time of a structure thus avoiding large maintenance or replacement expenses.

Lead extrusion energy dissipaters were proposed as a repeatable way of absorbing energy but the large size of these devices limited their use to certain applications such as base isolation (Cousins and Porritt 1993). Further research (Rodgers *et al.* 2007, Rodgers *et al.* 2007) led to the design and manufacture of a new generation of smaller extrusion devices also known as high-force-to-volume (HF2V) dampers. HF2V devices maintain the same level of force as their predecessors, but in much smaller dimensions and can thus easily fit into structural connections (Bacht *et al.* 2011). The device consists of a steel cylindrical container filled with lead and a moving bulged shaft passing through its axis as shown in Fig. 1. The HF2V behaviour may be modelled using a velocity-dependent nonlinear relation (Rodgers *et al.* 2008)

$$F_D = C_\alpha \left|\dot{y}\right|^\alpha \tag{1}$$

where F_D is the damper force, α is the velocity exponent, which is within the range of [0.11-0.15], C_α is the geometry dependent damper constant, and $\dot{y}$ is the shaft velocity.

Low cost and relative ease of manufacture together with their small size make HF2V devices a suitable option for wide use in the structures either in the design stage of new

*Corresponding author, Ph.D. Student
E-mail: farzin.golzar@pg.canterbury.ac.nz
[a]Associate Professor
[b]Professor

ISSN: 1225-4568 (Print), 1598-6217 (Online)

Fig. 1 Prototype lead extrusion damper (Rodgers *et al.* 2007) (left) and prototype friction ring spring (Hill 1995) (right)

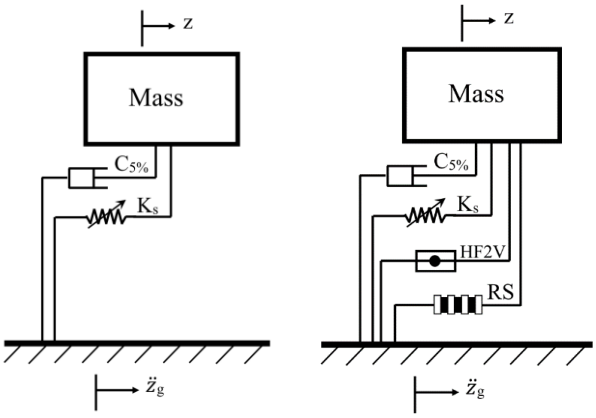

Fig. 2 Schematic configuration of a SDOF system and ground motion input. Left: uncontrolled; Right: controlled (with supplemental devices)

buildings or as a retrofit strategy (Rodgers *et al.* 2012). However, the absence of a self-centring force within these devices may result in residual displacements throughout the structure, particularly if the structural components deform beyond the elastic region (Kordani *et al.* 2015).

Ring springs are high-stiffness recentring springs which can be considered as fully passive friction dampers with high self-centring ability (Erasmus 1988, Hill 1995). As shown in Fig. 1 a ring spring essentially consists of a stack of inner and outer rings with tapered mating surfaces. As the stack is compressed, the inner rings are radially compressed and contracted, while the outer rings radially expand. This mechanism provides an extremely large stiffness in a relatively small size compared to other types of springs (Hill 1995). When the load is removed the rings return to their unloaded position giving the ring spring a self-centring ability.

Ring spring stiffness depends on the friction between sliding surfaces and is thus different in loading and unloading giving it a considerable measure of damping. The dissipative nature of the ring spring together with its inherent recentring ability makes it a favourable candidate for industrial applications where moderate, compact, and reliable energy absorption is needed (Kar *et al.* 1996, Filiatrault *et al.* 2000). Khoo *et al.* (2012) and Khoo *et al.* (2013) undertook experimental testing where they augmented a friction-based sliding hinge joint with a ring spring to provide restoring force and diminish the permanent displacements at the end of an earthquake shaking. These ring springs have also been used in the field, such as the Te Puni Village building that was constructed in 2008 in Wellington, New Zealand. This multi-storey steel-frame building included sliding friction connections, and ring springs which were located at the column-foundation connections, to allow damage-resistant rocking to occur (Gledhill *et al.* 2008). However, the use of these devices is still relatively uncommon and their potential in earthquake engineering is still largely unrealised.

Minimizing possible damage and/or repair costs is a common goal of structural design. To this end, determining maximum level of key response metrics including peak and residual displacement and peak base shear need to be thoroughly investigated and predicted. Minimizing peak structural displacement can reduce the deformation of individual structural components decreasing associated damage (Chiou *et al.* 2011, Ruiz-García and Aguilar 2015). Residual displacements are associated with post-event repair costs (Bazzurro *et al.* 2004, Luco *et al.* 2004, Polese *et al.* 2013, Salari and Asgarian 2015), but are often neglected in the design process. Finally, overall column force and total base shear force is directly related to required column strength and foundation demands (Elnashai *et al.* 2004).

This research aims to investigate the effects of using a supplemental hybrid HF2V plus ring spring damping device on the structural response parameters of a nonlinear structure. The structure has an elasto-plastic hysteretic behaviour thus exhibiting typical inelastic structural behaviour. The proposed hybrid device incorporates HF2V devices for their force capacity and dissipation and ring springs to add recentring. Nonlinear spectral analysis is done for a variety of HF2V and ring spring device capacities to parametrise their potential across a reasonable device design space in a form suitable for use in performance based design methods.

2. Modelling

A typical single-degree-of-freedom (SDOF) system for spectral analysis is shown in Fig. 2. Such models are regularly used in spectral analyses upon which performance based design codes rely (Chopra and Goel 2001, Subramanian and Velayutham 2014). In this case, the system includes a nonlinear elasto-plastic hysteresis for the structure and a supplemental damping system that is a hybrid of nonlinear HF2V and ring spring devices. The nonlinear structure is subjected to horizontal unidirectional seismic acceleration, $\ddot{z}_g$ with and without supplemental devices.

2.1 Nonlinear structure

Nonlinear elasto-plastic restoring force is modelled using the Menegotto-Pinto model (Menegotto and Pinto

1973)

$$F = \rho kz + \frac{(1-\rho)kz}{\left[1+\left|kz/F_Y\right|^{\beta}\right]^{1/\beta}} \tag{2}$$

where F is the structural force, z is the deformation, F_Y is the yield force, and k is the stiffness. The parameters ρ and β are used to define the shape of the curve, where ρ is the ratio of post-yield stiffness to pre-yield stiffness and β determines the shape of the transition curve.

2.2 HF2V dissipation device

The lead extrusion damper may be mathematically modelled using the Maxwell type mass-spring configuration (Rodgers *et al.* 2012). The total shaft displacement, z, is the sum of two separate components; linear elastic elongation of the device shaft, x, and the nonlinear bulge displacement within the cylinder, y, as in Fig. 3 yielding

$$x + y = z \tag{3}$$

Due to the series nature of the spring-damper model, the spring (representing the elastic deflection of the shaft) and damper have an equivalent force. Experimental results (Cousins *et al.* 1991, Rodgers *et al.* 2008) indicate this force is related to the shaft velocity

$$F_D = C_\alpha \left|\dot{y}\right|^{\alpha} = \frac{x}{f_D} \tag{4}$$

where α is the velocity exponent, C_α is the geometry dependent damper constant, and f_D is the spring flexibility. Combining Eqs. (3)-(4) yields

$$\left(\frac{F_D}{C_\alpha}\right)^{1/\alpha} = \dot{z} - f_D \dot{F}_D \tag{5}$$

Converting Eq. (5) to the finite difference form and rearranging the terms yields

$$\Delta t\left(\frac{F_{D,i+1}}{C_\alpha}\right)^{1/\alpha} + f_D F_{D,i+1} = z_{i+1} - z_i + f_D F_{D,i} \tag{6}$$

where i is the time index. Note that the right hand side of the equation consists of known parameters at each time step, t_i. To find F_D from Eq. (6), an iterative method is required. Thus, the equation is rewritten

$$F_{D,i+1} = C_\alpha \left(\frac{z_{i+1} - z_i + f_D F_{D,i}}{\Delta t + C_\alpha f_D F_{D,i+1}^{\,1-1/\alpha}}\right)^{\alpha} \tag{7}$$

Comparing Eq. (7) and Eq. (4), the bracketed term is indeed the shaft velocity at instance t_{i+1}. To avoid erroneous results due to the fractional exponent and also considering the direction of motion, Eq. (7) is broken into two separate parts

$$\dot{y}_{i+1} = \frac{z_{i+1} - z_i + f_D F_{D,i}}{\Delta t + C_\alpha f_D F_{D,i+1}^{\,1-1/\alpha}} \tag{8}$$

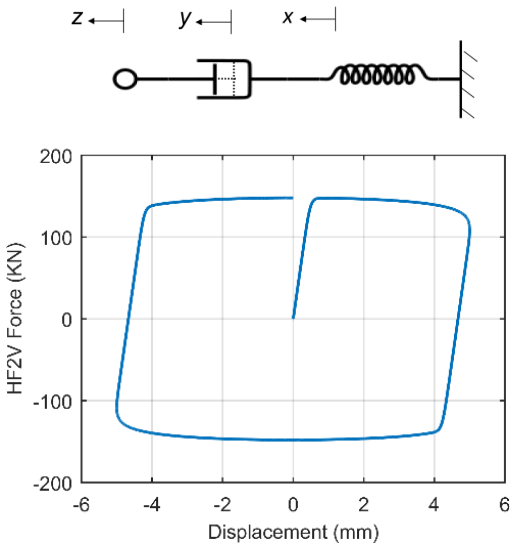

Fig. 3 Schematic configuration (top) and force-displacement behavior of a HF2V device (bottom)

$$F_{D,i+1} = C_\alpha \left|\dot{y}_{i+1}\right|^{\alpha} \times sign\left(\dot{y}_{i+1}\right) \tag{9}$$

Using sufficiently small time increments and a sufficient number of iterations in each step, Eqs. (8)-(9) will yield F_D. The resulting force-displacement behaviour shown in Fig. 3 (Rodgers *et al.* 2011) is in agreement with finite elements results of Yang *et al.* (2015).

2.3 Friction ring spring

To model the behaviour of a stacked ring spring, a single ring is isolated to show the forces acting on an inner ring, as shown in Fig. 4. Since the direction of the friction force depends on the direction of axial motion, the relation between the axial force and axial displacement of the ring, which represents the axial stiffness, will be different depending on whether the rings are moving apart (unloading) or the gap between them is closing (loading). It can be proved that the ratio of the increasing axial stiffness to the decreasing axial stiffness is defined (Erasmus 1988)

$$\frac{K_d}{K_i} = \frac{(\mu - \tan(\alpha))(1 - \mu\tan(\alpha))}{(1 + \mu\tan(\alpha))(\mu + \tan(\alpha))} \tag{10}$$

where K_d is the decreasing (unloading) stiffness and K_i is the increasing (loading) stiffness. Fig. 4 also shows the typical behaviour of a ring spring in terms of force-displacement diagram.

As expected, increasing stiffness is always greater than the decreasing stiffness. However, the stiffness and the total displacement capacity of the ring spring may be manipulated by using a different number of rings in a stack, using different configurations (parallel or series) of ring springs, and utilising different lubricants to lower the frictional coefficient (Hill 1995). As evident in Fig. 4, the displacement corresponding to zero force is zero. This result ensures self-centring, which is an important characteristic of these devices and proves useful in managing nonlinear seismic displacements.

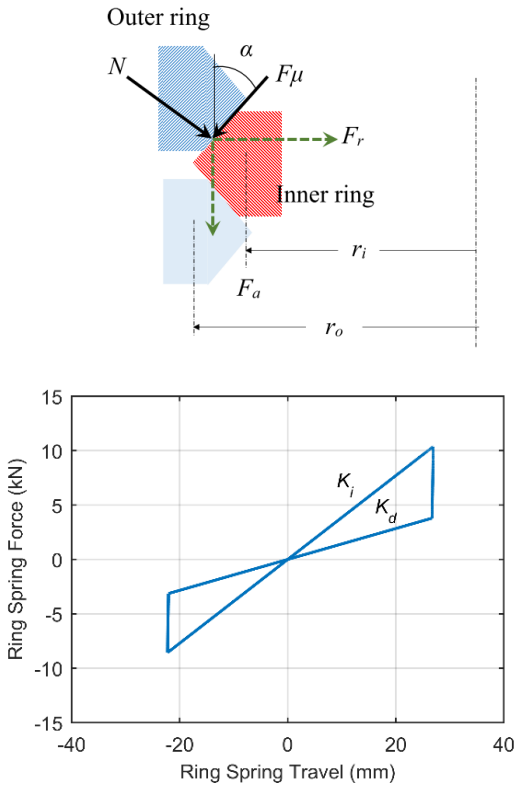

Fig. 4 Resolved forces on the inner ring (top) and force-displacement behaviour of a ring spring device (bottom)

2.4 Hybrid device

Combining the high dissipation of a HF2V device and the recentring ability of a ring spring, may provide benefits over using each component alone. However, the nonlinear nature of these devices precludes a direct formulation to predict their behaviour in a structure. While the nonlinearity of ring spring dynamics is the result of its direction-dependent multi-value stiffness, the nonlinearity of HF2V is because of its velocity-dependent force. The combination of such behaviours makes the design process more complicated.

Eq. (11) shows the governing equation of motion for the system shown in Fig. 2 including this hybrid device

$$m_e\ddot{z} + c\dot{z} + F_{NL} + F_{RS} + F_{HF2V} = -m_e\ddot{z}_g \tag{11}$$

where m_e is the seismic mass of the structure, F_{NL} is the nonlinear structural restoring force, F_{RS} is the ring spring force, and F_{HF2V} is the lead-extrusion damper force.

The impact of each component on the overall behaviour of the hybrid device depends on their design parameters. The HF2V contribution is defined by ε, which is defined as the ratio of peak HF2V force C_α in Eq. (4) to the seismic weight, $m_e g$ at a reference velocity of 1.0 m/s, giving

$$C_\alpha = \varepsilon m_e g \tag{12}$$

Moreover, the value α=0.12 is used in Eq. (4) based on the experimental results (Cousins and Porritt 1993, Rodgers *et al.* 2006, Rodgers *et al.* 2007). The ring spring force can be specified by its loading and unloading stiffness values (K_i and K_d). A convenient way is to specify them as a percentage of pre-yield structural stiffness, K_s.

Table 1 Ground motion records used in the simulations (medium suite of records in SAC project)

No.	SAC No.	Record name	PGA (g)
1	(la01)	Imperial Valley,	0.46
2	(la02)	Imperial Valley,	0.68
3	(la03)	Imperial Valley, 1979, Array 5	0.39
4	(la04)	Imperial Valley, 1979, Array 5	0.49
5	(la05)	Imperial Valley, 1979, Array 6	0.30
6	(la06)	Imperial Valley, 1979, Array 6	0.23
7	(la07)	Landers Eqk, 1992	0.42
8	(la08)	Landers Eqk, 1992	0.43
9	(la09)	Landers Eqk, 1992	0.52
10	(la10)	Landers Eqk, 1992	0.36
11	(la11)	Loma Prieta, 1989, Gilroy	0.67
12	(la12)	Loma Prieta, 1989, Gilroy	0.97
13	(la13)	Northridge, 1994	0.68
14	(la14)	Northridge, 1994	0.66
15	(la15)	Northridge, 1994	0.53
16	(la16)	Northridge, 1994	0.58
17	(la17)	Northridge, 1994, Sylmar	0.57
18	(la18)	Northridge, 1994, Sylmar	0.82
19	(la19)	North Palm Springs, 1986	1.02
20	(la20)	North Palm Springs, 1986	0.99

2.5 Analyses

To investigate the impact of hybrid devices over a design space of non-dimensional damper capacity, ε and K_i/K_s, a nonlinear spectral analysis (Ewing *et al.* 2009, Maniyar *et al.* 2009) is conducted using the medium suite of design level earthquakes (shown in Table 1) from the SAC project (Somerville and Venture 1997). This suite includes 20 acceleration time histories with a probability of exceedance of 10% in 50 years. The results can then be used to assess the reductions in structural response, base shear demand, and residual displacement, parametrised by the device design parameters ε and K_i/K_s over a full range of structural periods to ensure easy integration into performance based design.

The model is presumed to have a nominal height, H_e=10 m, a seismic mass, m_e=10^4 Kg with the pre-yield structural stiffness determined by the natural period of the uncontrolled structure, (K_s=2π m_e^2/T). A yield drift value of δ_y=2% together with parameters ρ=5% and β=20 in Eq. (2) are used to model the nonlinear structural stiffness. To account for elastic dissipation losses, inherent structural damping equal to 5% of critical damping is considered. The nonlinear time history response of the structure is evaluated for the selected hybrid device configurations using the software package MATLAB. Peak response parameters including displacement and base shear are recorded together with the residual displacement at the end of oscillation.

The data extracted from the time history response of 20

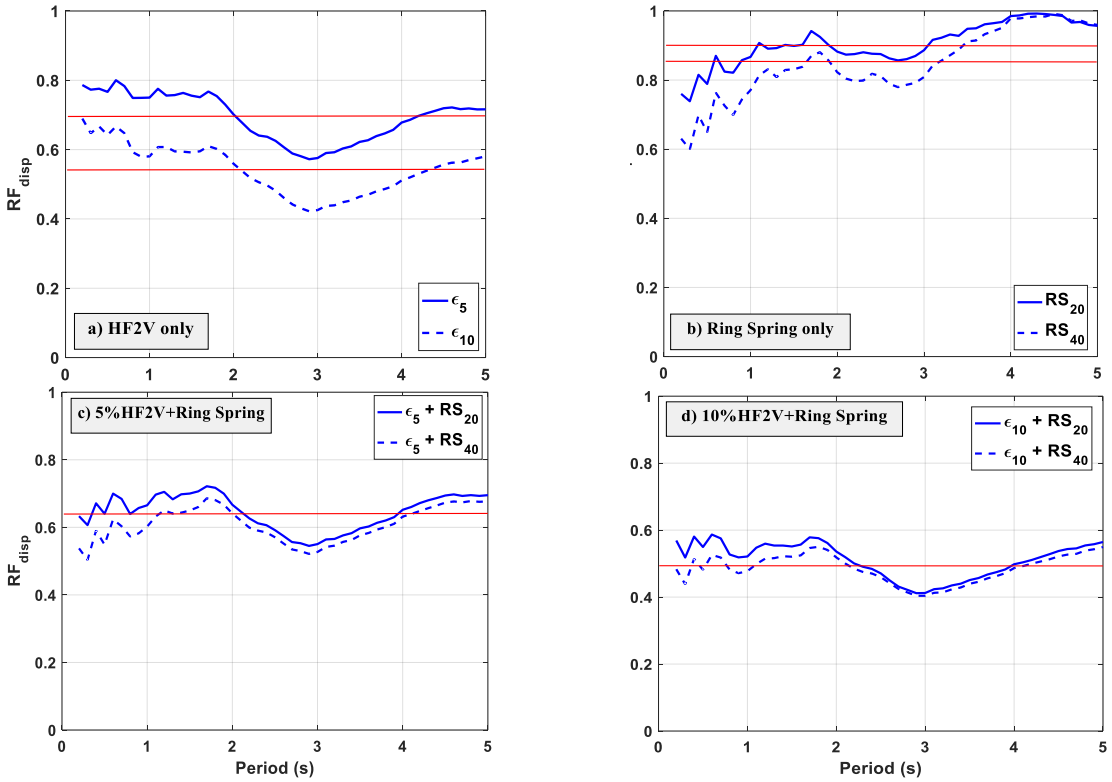

Fig. 5 Displacement RF results for: (a) HF2V only; (b) Ring Spring only; (c) 5% HF2V with both ring springs; and (d) 10% HF2V with both ring springs. Solid horizontal lines show average values for the results across all periods

earthquake records is used to evaluate the statistically representative metrics for each structural period. In accordance with the log-normal distribution of results, geometric mean values are used to show the average values of peak displacement and peak base shear, and median values are used for residual displacements. This process is repeated for structural periods in the range T_n=[0.2-5] (s) with an increment dT=0.1 (s) to provide the response spectra (Maniyar *et al.* 2009).

To better demonstrate how the supplemental damping alters the behaviour of a structure, the results are shown in the form of reduction factors. A reduction factor for a particular response metric is defined as a ratio of the modified structure response with added device to the uncontrolled structure response without device. As such, a value lower than 1.0 indicates a reduction in response (Bhunia *et al.* 2012).

The response spectra are created for a set of parametrised hybrid device configurations. Two values of ε=5% and ε=10% are used to study the effect of HF2V capacity based on previous research (Rodgers *et al.* 2008). Two different ring spring scenarios, RS_{20} and RS_{40}, characterised by loading stiffness values of K_i/K_s=20% and K_i/K_s=40% are considered in the analyses, where K_s is the pre-yield structural stiffness. For both ring springs, the unloading stiffness is considered to be 35% of the loading stiffness (K_d/K_i=35%), so RS_{20} and RS_{40} have the return stiffness ratios of 7% and 14% respectively.

The values of 5% and 10% storey weight for the HF2V device force capacity are defined from prior analyses done on steel beam-column connections (Rodgers *et al*. 2007). They are achievable device forces offering significant reductions and provide values below the equivalent plastic moment capacity of the beam depending on how it is specifically connected to the structure (Bacht *et al.* 2011). The ring springs are similarly scaled as a percentage of system stiffness to parametrise them to the structural design parameters. The values of 20% and 40% loading stiffness and respective return stiffnesses of 7% and 14%, as shown in Fig. 4, are regarded in design as levels that enable recentring of structures (Khoo *et al.* 2012). Thus, these values were chosen based on the recentring stiffness they would offer as that was the primary reason for their use. However, a very wide range of possibilities is available, but these parameterised choices display the potential range of response achievable with typically available device capacities over the range of structural periods considered.

Each of the four components of ε_5, ε_{10}, RS_{20}, and RS_{40} are utilized in the structural model separately and in combination to generate 8 hybrid device configurations with 3 spectral analysis plots (RF_{disp}, RF_{shear}, RF_{res}) for each configuration. The overall results should fully characterise the design specifications and relative impact of these devices. Such spectra can thus provide design input to performance based design methods.

3. Spectral analyses results

3.1 Displacement

The reduction factors (RFs) for displacement response

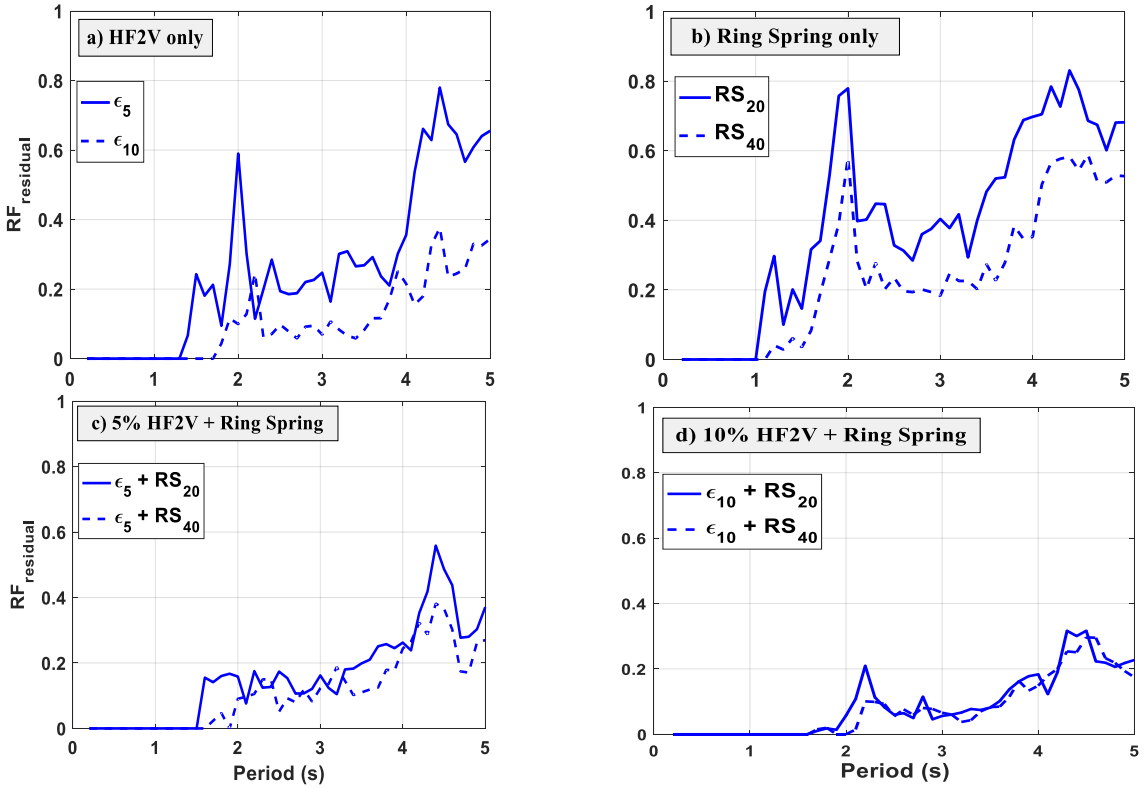

Fig. 6 Residual displacement RF results for: (a) HFV2 only; (b) Ring Spring only; (c) 5% HF2V with both ring springs; and (d) 10% HF2V with both ring springs

are shown in Fig. 5. The HF2V device significantly decreases the peak displacement results (Fig. 5(a)) with an average 30% reduction for ε_5 and 45% reduction for ε_{10} whereas only a 10-15% average reduction is seen for RS_{20} and RS_{40} (Fig. 5(b)). The combination of 5% HF2V and ring springs ($RS_{20,}$ RS_{40}) results in the RFs shown in Fig. 5(c). An average value of 0.6 is obtained for the total period range with the difference between RS_{20} and RS_{40} being reasonably insignificant particularly for periods greater than 2 sec. Reduction factors for ε_{10} and two ring springs show a similar trend to those of ε_5 (Fig. 5(d)), but with a further increase in displacement reductions (RF_{disp}=0.5). The relatively small difference between the results of the hybrid device with different ring spring sizes suggests that the use of larger ring springs would not be fully justified based on displacement reductions alone. Overall, HF2V devices provide the primary reductions in peak displacement, where Fig. 5(a) results are in accordance with the linear spectral analyses of Rodgers *et al.* (2008).

3.2 Residual displacement

Residual displacement RFs are shown in Fig. 6. Reduced residual displacements with only HF2V (Fig. 6(a)) are mainly due to the overall decreased displacements throughout the time history. However, the reductions resulted using only ring spring (Fig. 6(b)) are associated with recentring stiffness and the reduced displacement due to the damping from the ring springs. Hybrid devices, show markedly greater average reductions higher than 80%, combining the positive effects of HF2V and ring spring (Figs. 6(c)-(d)). If the residual displacement is important, then a larger ring spring is more favourable as it provides greater recentring.

3.3 Base shear

Base shear RFs are shown in Fig. 7 where a reduction in base shear is observed for structures with periods less than approximately 1 sec. However, for longer period structures, significantly increased base shear is observed, as a consequence of the resistive and restoring forces imposed by the supplemental components. Such an increase suggests that the forces added to reduce displacements outweigh the reduced structural forces due to those displacement reductions. Comparing the response spectra with and without HF2V shows that the base shear is largely dominated by the contribution of the HF2V devices due to their dominant contribution to displacement reductions in Fig. 5. In addition, the added base shear in the case of the structure with ring spring only, is largely independent of its natural period.

To determine the contribution of individual components to the maximum base shear, percentage share of each component (nonlinear structural restoring force [F_S], HF2V force [F_{HF2V}], and ring spring force [F_{RS}]) to the overall base shear is shown in Fig. 8. The plots are generated similar to the way response spectra were created and shown in previous figures i.e., the contribution of each component at the instance of maximum base shear during a particular ground motion input is recorded. Then the data obtained from all 20 earthquakes are then plotted using geometric

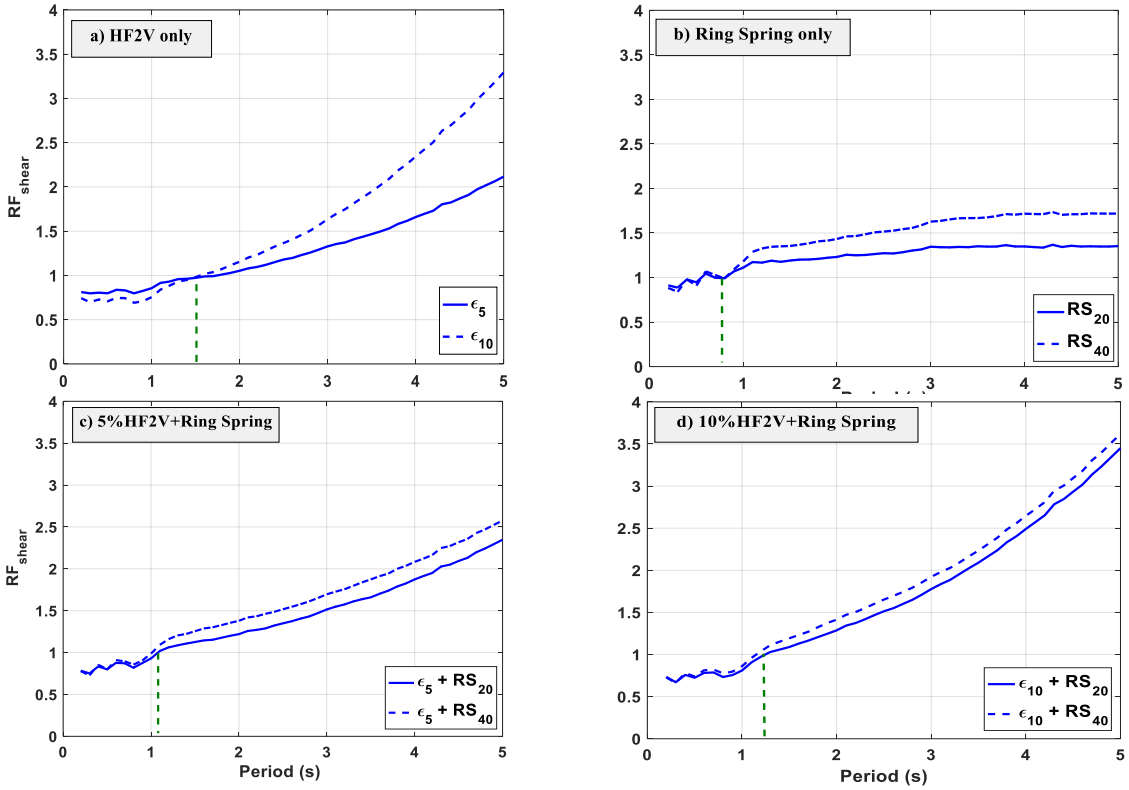

Fig. 7 Base shear RF results for: (a) HFV2 only; (b) Ring Spring only; (c) 5% HF2V with both ring springs; and (d) 10% HF2V with both ring springs. Green vertical dashed lines show the period for RF_{shear}=1

mean values.

A period-dependent increasing trend is witnessed for the HF2V force which is mainly associated with its velocity-dependent behaviour (Figs. 8(a) and 8(c)-(d)). The relative contribution of structural restoring force decreases as the period of the structure gets longer since the structural stiffness of the system decreases with an increase in natural period. Moreover, the base shear contribution of the ring spring in the hybrid device shows relatively low sensitivity to the natural period of the structure with ~15% for RS_{20} and ~20% for RS_{40}.

3.4 Summary discussion

Displacement response reductions are mainly dominated by the effect of HF2V device indicating that using larger device (ε_{10}) without ring spring is favourable based on displacement alone. However, with regards to residual displacement, both components show a robust performance. Results suggest that an excellent reduction in residual displacement is achieved by using a hybrid device reducing the need for any post-earthquake remediation on a structure using these devices.

However, reductions come at a cost. Base shear response is dominated by the contribution of HF2V force and ring springs impose the smaller forces to the structure. Considering base shear alone, the smaller ring spring only (RS_{20}) is the best option to add to the structure. Considering all three response parameters evaluated, using a hybrid device that consists of 5% HF2V device (ε_5) and 40% ring spring (RS_{40}) seems to generate a more optimal response spectra for performance versus increased base shear. The overall results allow any series of choices to be assessed parametrically as the stiffness ratios and ε values span a reasonably achievable range for these devices (Rodgers *et al.* 2007, Rodgers *et al.* 2008, Khoo *et al.* 2013, Bishay-Girges and Carr 2014).

The SDOF design spectrum analysis is limited by the number of degrees of freedom. However, the analysis approach using RFs is entirely generalizable. For multi-degree-of-freedom (MDOF) systems representing multi-storey structures the reduction factors would be calculated in a similar fashion but there would be more of them depending on the number of storeys. For displacement at every storey of an 8-storey frame, there would be 8 RFs. However, if the structure was first mode dominant in response, as is typical, then the top storey deflection and single RF, similar to this analysis would suffice. In this case, any complex MDOF case is often quite specific to a single structure, where the approach here is generalizable to initial design of many possible structures. The analysis of how these devices influence the response of larger MDOF structures in the presence of higher mode effects is an important aspect of future work.

Experimental verification is critical. However, this paper first establishes the potential for these hybrid devices before engaging in an extensive experimental test series. Because they are hybrid devices, experimental outcomes for a given device is the combination of the force capacities of both devices as a function of the input displacement and velocity. Thus, while a hybrid device has not been experimentally validated, there is extensive device level and

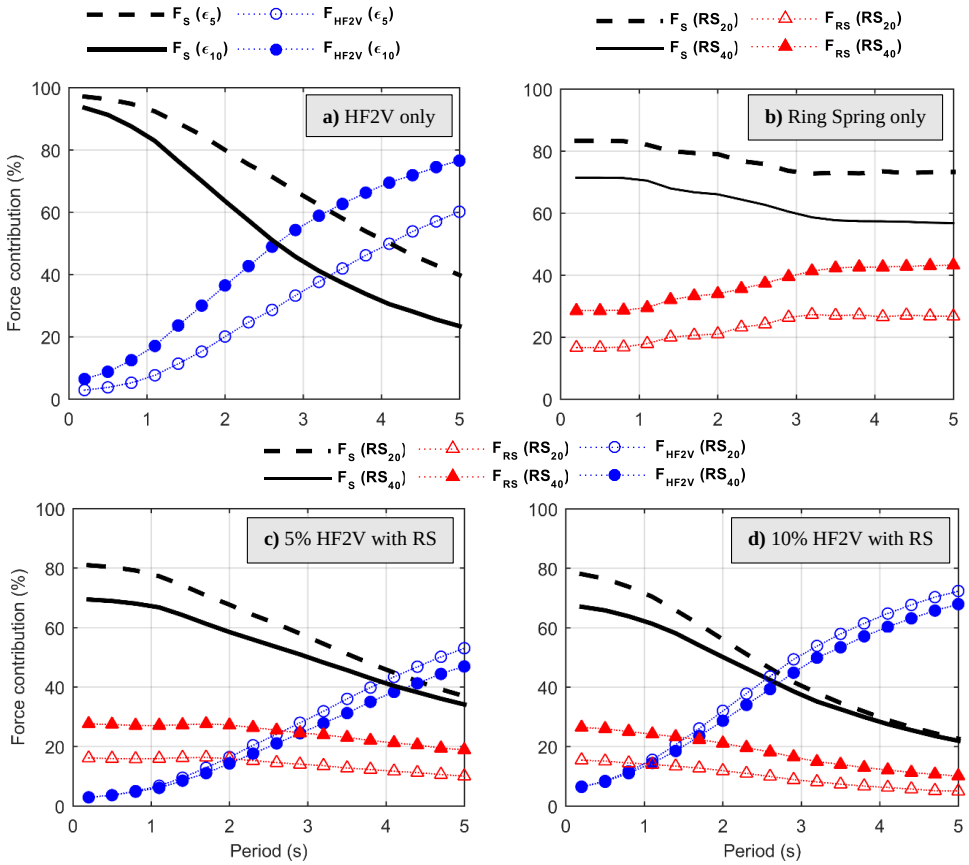

Fig. 8 Base shear components: (a) HFV2 only; (b) Ring Spring only; (c) 5% HF2V with both ring springs; and (d) 10% HF2V with both ring springs

in-situ validation of HF2V devices (Rodgers *et al.* 2008) and of ring springs (Khoo *et al.* 2012, Khoo *et al.* 2013). These outcomes show that the devices behave according to the models used in this paper in Eqs. (3)-(10) for modelling them. Thus, while the paper does not include experimental validation of a hybrid device, there is confidence that upcoming validation experiments, which were outside the length and scope of this article, will behave similarly.

4. Conclusions

Comprehensive simulation of the structural response of a nonlinear hysteretic structure across a range of earthquakes has shown that significant reductions in peak displacement response can be achieved using realistic configurations of hybrid damping devices. Based on the investigations described, the following conclusions can be drawn:

- Both the HF2V device and ring spring can modify the response metrics of the nonlinear system in terms of peak and residual displacements as a result of their damping capacity.
- Peak displacement reduction factors are mainly controlled by the impact of HF2V devices particularly for larger periods.
- Separately, either HF2V devices or ring springs reduce the residual displacements. However, combining them in a hybrid device results in even greater reductions of residual displacements giving the structure high self-centring ability.
- Using supplemental damping devices can result in reduced base shear force only for low period structures. For higher periods, noticeably magnified base shear forces are witnessed in the structure.
- The increase in base shear is dominated by the contribution of HF2V component. Thus, from the base shear point of view, smaller HF2V is preferred for a hybrid device.
- Using ring spring only results in considerably lower residual displacements, with minimal increase in base shear. Thus, from a residual displacement viewpoint, using ring spring only is preferred over a hybrid device.

References

Bacht, T., Chase, J.G., MacRae, G., Rodgers, G.W., Rabczuk, T., Dhakal, R.P. and Desombre, J. (2011), "HF2V dissipator effects on the performance of a 3 story moment frame", *J. Constr. Steel Res.*, **67**(12), 1843-1849.

Bazzurro, P., Cornell, C., Menun, C. and Motahari, M. (2004). "Guidelines for seismic assessment of damaged buildings", *Proceedings of the 13th World Conference on Earthquake Engineering*, Vancouver, Canada.

Bhunia, D., Prakash, V. and Pandey, A.D. (2012), "A study on the behaviour of coupled shear walls", *Struct. Eng. Mech.*, **42**(5),

645-675.

Bishay-Girges, N.W. and Carr, A.J. (2014), "Ring spring dampers: Passive control system for seismic protection of structures", *Bull. NZ. Soc. Earthq. Eng*., **47**(3).

Chang, S.E. (2010), "Urban disaster recovery: a measurement framework and its application to the 1995 Kobe earthquake", *Disast*., **34**(2), 303-327.

Chiou, D.J., Hsu, W.K., Chen, C.W., Hsieh, C.M., Tang, J.P. and Chiang, W.L. (2011), "Applications of Hilbert-Huang transform to structural damage detection", *Struct. Eng. Mech*., **39**(1), 1-20.

Chopra, A.K. and Goel, R.K. (2001), "Direct displacement-based design: use of inelastic vs. elastic design spectra", *Earthq. Spectra*, **17**(1), 47-64.

Cousins, W. and Porritt, T. (1993), "Improvements to lead-extrusion damper technology", *Bull. NZ. Nat. Soc. Earthq. Eng*., **26**(3), 342-348.

Cousins, W., Robinson, W. and McVerry, G. (1991). "Recent developments in devices for seismic isolation", *Proc. Pacific Conference on Earthquake Engineering*.

Elnashai, A.S., Borzi, B. and Vlachos, S. (2004), "Deformation-based vulnerability functions for RC bridges", *Struct. Eng. Mech*., **17**(2), 215-244.

Erasmus, L. (1988), "Ring springs on holding-down bolts for seismic energy dissipation", *Tran. Inst. Prof. Eng. NZ: Civil Eng. Sec.*, **15**(2), 41-47.

Ewing, C.M., Guillin, C., Dhakal, R.P. and Chase, J.G. (2009), "Spectral analysis of semi-actively controlled structures subjected to blast loading", *Struct. Eng. Mech*., **33**(1), 79-93.

Filiatrault, A., Tremblay, R. and Kar, R. (2000), "Performance evaluation of friction spring seismic damper", *J. Struct. Eng*., **126**(4), 491-499.

Gledhill, S., Sidwell, G. and Bell, D. (2008). "The damage avoidance design of tall steel frame buildings-Fairlie terrace student accommodation project, Victoria University of Wellington", *New Zealand Society of Earthquake Engineering Annual Conference*.

Hamid, N.H. and Mander, J. (2014), "Damage avoidance design for buildings", *KSCE J. Civil Eng.*, **18**(2), 541-548.

Hill, K.E. (1995), *The Utility of Ring Springs in Seismic Isolation Systems: A Thesis Submitted for the Degree of Doctor of Philosophy*, University of Canterbury, New Zealand.

Kaiser, A., Holden, C., Beavan, J., Beetham, D., Benites, R., Celentano, A., Collett, D., Cousins, J., Cubrinovski, M. and Dellow, G. (2012), "The Mw 6.2 Christchurch earthquake of February 2011: preliminary report", *NZ J. Geol. Geophys*., **55**(1), 67-90.

Kar, R., Rainer, J. and Lefrançois, A. (1996), "Dynamic properties of a circuit breaker with friction-based seismic dampers", *Earthq. Spectra*, **12**(2), 297-314.

Khoo, H.-H., Clifton, C., Butterworth, J. and MacRae, G. (2013), "Experimental study of full-scale self-centering Sliding Hinge Joint connections with friction ring springs", *J. Earthq. Eng*., **17**(7), 972-997.

Khoo, H.-H., Clifton, C., Butterworth, J., MacRae, G., Gledhill, S. and Sidwell, G. (2012), "Development of the self-centering Sliding Hinge Joint with friction ring springs", *J. Constr. Steel Res*., **78** 201-211.

Khoo, H., Clifton, G., Butterworth, J. and MacRae, G. (2012). "Experimental studies of the self-centering Sliding Hinge Joint", *NZSEE Conference*, Christchurch, New Zealand.

Kordani, R., Rodgers, G. and Chase, J. (2015). "Response analysis of hybrid damping device with self-centring", *New Zealand Society of Earthquake Engineering Conference*.

Luco, N., Bazzurro, P. and Cornell, C.A. (2004). "Dynamic versus static computation of the residual capacity of a mainshock-damaged building to withstand an aftershock", *Proceedings of the 13th World Conference on Earthquake Engineering*.

Mander, J.B. and Cheng, C.-T. (1997), *Seismic Resistance of Bridge Piers based on Damage Avoidance Design*, U.S. National Center for Earthquake Engineering Research (NCEER).

Maniyar, M.M., Khare, R.K. and Dhakal, R.P. (2009), "Probabilistic seismic performance evaluation of non-seismic RC frame buildings", *Struct. Eng. Mech*., **33**(6), 725-745.

Menegotto, M. and Pinto, P. (1973), *Method of Analysis for Cyclically Loaded R. C. Plane Frames Including Changes in Geometry and Non-Elastic Behavior of Elements under Combined Normal Force and Bending*,

Polese, M., Di Ludovico, M., Prota, A. and Manfredi, G. (2013), "Damage-dependent vulnerability curves for existing buildings", *Earthq. Eng. Struct. Dyn*., **42**(6), 853-870.

Rodgers, G., Denmead, C., Leach, N., Chase, J. and Mander, J. (2006), "Spectral evaluation of high force-volume lead dampers for structural response reduction".

Rodgers, G.W., Chase, J.G., Mander, J., Dhakal, R.P. and Solberg, K.M. (2007). "DAD Post-Tensioned Concrete Connections with Lead Dampers: Analytical Models and Experimental Validation", *8th Pacific Conference on Earthquake Engineering*.

Rodgers, G.W., Chase, J.G., Mander, J.B., Leach, N.C. and Denmead, C.S. (2007), "Experimental development, tradeoff analysis and design implementation of high force-to-volume damping technology", *Bull. NZ Soc. Earthq. Eng*., **40**(2), 35-48.

Rodgers, G.W., Mander, J.B. and Chase, J.G. (2011), "Semi-explicit rate-dependent modeling of damage-avoidance steel connections using HF2V damping devices", *Earthq. Eng. Struct. Dyn.*, **40**(9), 977-992.

Rodgers, G.W., Mander, J.B., Chase, J.G., Dhakal, R.P., Leach, N.C. and Denmead, C.S. (2008), "Spectral analysis and design approach for high force-to-volume extrusion damper-based structural energy dissipation", *Earthq. Eng. Struct. Dyn*., **37**(2), 207-223.

Rodgers, G.W., Solberg, K.M., Chase, J.G., Mander, J.B., Bradley, B.A., Dhakal, R.P. and Li, L. (2008), "Performance of a damage-protected beam-column subassembly utilizing external HF2V energy dissipation devices", *Earthq. Eng. Struct. Dyn*., **37**(13), 1549-1564.

Rodgers, G.W., Solberg, K.M., Mander, J.B., Chase, J.G., Bradley, B.A. and Dhakal, R.P. (2012), "High-force-to-volume seismic dissipators embedded in a jointed precast concrete frame", *J. Struct. Eng.*, **138**(3), 375-386.

Ruiz-García, J. and Aguilar, J.D. (2015), "Aftershock seismic assessment taking into account postmainshock residual drifts", *Earthq. Eng. Struct. Dyn*., **44**(9), 1391-1407.

Salari, N. and Asgarian, B. (2015), "Seismic response of steel braced frames equipped with shape memory alloy-based hybrid devices", *Struct. Eng. Mech*., **53**(5), 1031-1049.

Somerville, P.G. and Venture, S.J. (1997), *Development of Ground Motion Time Histories for Phase 2 of the FEMA/SAC Steel Project*, SAC Joint Venture

Subramanian, K. and Velayutham, M. (2014), "Seismic performance of lateral load resisting systems", *Struct. Eng. Mech*., **51**(3), 487-502.

Yang, M., Xu, Z. and Zhang, X. (2015), "Experimental study on lead extrusion damper and its earthquake mitigation effects for large-span reticulated shell", *Steel Compos. Struct.*, **18**(2), 481-496.

Yon, B., Sayın, E. and Koksal, T.S. (2013), "Seismic response of buildings during the May 19, 2011 Simav, Turkey earthquake", *Earthq. Struct*., **5**(3), 343-357.

CC